Available online at www.sciencedirect.com

ScienceDirect

Journal of the European Ceramic Society 34 (2014) 3389–3398

www.elsevier.com/locate/jeurceramsoc

# Influence of pyrolysis temperature on fracture response in SiOC based composites reinforced by basalt woven fabric

Zdeněk Chlup [a,*], Martin Černý [b], Adam Strachota [c], Zbyněk Sucharda [b], Martina Halasová [a,d], Ivo Dlouhý [a]

[a] CEITEC IPM, Institute of Physics of Materials, v.v.i., Academy of Sciences of the Czech Republic, Brno, Czech Republic
[b] Institute of Rock Structure and Mechanics, v.v.i., Academy of Sciences of the Czech Republic, Prague, Czech Republic
[c] Institute of Macromolecular Chemistry, v.v.i., Academy of Sciences of the Czech Republic, Prague, Czech Republic
[d] Institute of Materials Science and Engineering, Faculty of Mechanical Engineering, Brno University of Technology, Brno, Czech Republic

Available online 1 April 2014

**Abstract**

The fracture resistance of ceramic based composites reinforced by various ceramic fibres can be dramatically enhanced when an efficient fracture mechanism takes place during the crack propagation. Presented work shows an effect of the pyrolysis temperature of the composite matrix on the fracture behaviour of the composite. The matrix is formed from the polysiloxane resin precursor and the reinforcement is a basalt woven fabric. The temperature range under investigation was from 600 °C, where the onset of fracture properties were observed up to 800 °C. Above this temperature basalt fibres suffer by rapid degradation of the microstructure. The optimum stage of the polysiloxane resin transformation maximizing the fracture resistance of the composite was identified. The fractographic analysis of the fracture surfaces revealed the differences in the acting fracture mechanism.


*Keywords:* Fracture behaviour; CMCs; Pyrolysis; Basalt fibre; Polysiloxane

## 1. Introduction

Composite materials using long fibres as a reinforcement are widely used in many applications. The majority of such composites use a polymer matrix reinforced by long fibres and usually are used in the shell form, e.g. airframes, car body, windmills, building parts etc., and they are known as fibre reinforced polymers (FRP) or more specifically utilizing carbon fibres (CFRP) and glass fibres (GFRP). The fibres can be arranged unidirectionally or most frequently in the form of 2D woven fabric or for special applications in the form of 3D woven fabric. The unidirectional reinforcement possesses the best utilisation of fibres when uniaxial external loading in the direction of fibres axes of the composite material is applied. However, the majority of applications suffer by the presence of combined loading (multiaxial) and therefore usually 2D woven fabric is used instead. The employment of 2D woven fabric can ensure ability of the composite material to offer appropriate biaxial (in plane) properties which are, however, lower than properties obtained in the case of uniaxially reinforced composite materials in preferred orientation.[1–7] It is given by lower number of acting fibres compared to the unidirectional composite in each direction when 2D reinforcement is used. Polymer based matrices are used thanks to their good workability, shaping and good ratio between price and properties. The main disadvantage can be seen in the low resistance to high temperatures of such matrix given by the polymer glass transition temperature and partially also by the fibres used and the environment influence. The glass transition temperature is for most of used polymers between 65 and 120 °C. However, the application temperature of FRP composites can be higher in some cases but it should not exceed temperature between 200 and 300 °C for long exposition time.[8,9] The limiting part of FRP composites is the polymeric matrix. On the other hand the ceramic matrix composites (CMCs) reinforced by long fibres are able to sustain long term exposition to temperatures above 1000 °C together with higher strength and stiffness. The weak point of CMCs is their low fracture resistance and many times higher production price given partly by expensive raw materials

* Corresponding author. Tel.: +420 532 290 335; fax: +420 541 218 657.
*E-mail address:* chlup@ipm.cz (Z. Chlup).

http://dx.doi.org/10.1016/j.jeurceramsoc.2014.03.003
0955-2219/

and by energy demanding processing. The CMCs reinforced by the long fibres are predominantly used in advanced applications for highly loaded parts in the airspace, military and chemical industry. The gap between cheap, reliable FRPs and expensive, brittle CMCs can be filled by hybrid composites. Many authors try to bring advantages from the polymeric and ceramic world together. SiOC glass prepared by the pyrolysis (thermochemical decomposition) of polysiloxane based resins possesses excellent thermal stability at temperatures up to 1500 °C.[10–16] The SiOC based glasses can be modified by changing of chemistry of precursors allowing preparation of composites where no fibre treatment such as a coating is necessary. This fact simplifies the processing of the composite significantly.[17–20] Other possible way of adjusting the interface bonding between matrix and fibres is application of partial pyrolysis where polymeric chains are not completely transformed to the fully amorphous SiOC glass as was reported elsewhere.[21–26] The material prepared by the partial pyrolysis has limited temperature of application which is close to the temperature of the pyrolysis. Therefore the application of high temperature resistance ceramic fibres (e.g. Nextel 720) is not worthwhile and usage of basalt fibres seems to be more effective solution.[27,28] The advantage of the basalt fibres application is their availability and low price comparing to the ceramic fibres. Additionally, it was proved in previous works that by the application of the partial pyrolysis of polysiloxane resins high fracture resistance, appropriate strength and good thermal stability controlled by properties of the fibres and degree of transformation during the pyrolysis can be achieved. The good fracture resistance can be achieved only when effective toughening mechanisms take place during the fracture process. A number of toughening mechanisms is known (i.e. crack bridging, crack deflection, fibre pull-out, micro-cracking shielding, delamination etc.), however, only their optimal combination can lead to the expected result.[29–31] The fibre matrix interface plays the key role determining how effective the given mechanism will be. When mainly fibre pull-out is acting, the fracture toughness can be significantly increased in the case of unidirectional fibre reinforced ceramic composites. This study uses two kinds of commercially available resins to demonstrate influence of the matrix precursor and the basalt 2D woven fabric with the orientation 0°/90°. The effect of the partial pyrolysis on the resulting properties determined at static and dynamic loading will be expressed. Also results from the fractographic analysis will be discussed in detail.

## 2. Materials and methods

Two polymeric precursors based on siloxane for a composite matrix were selected, i.e. polymethylsiloxane resin – MS (Lukosil M130) and polymethylphenylsiloxane resin – MPS (Lukosil 901) both produced by Lučební závody Kolín, Czech Republic. The partial polymer-to-ceramic thermochemical transformation was done by the pyrolysis within the temperature range between 600 °C and 800 °C with the step of 50 °C. The basalt plain woven fabric having area weight of 186 g m$^{-2}$, thread count ratio (warp/weft) of 100/75 produced by VÚLV, spol. s.r.o. Czech Republic was used as a reinforcement. Measured parameters of the basalt roving used for the manufacturing of the fabric were following: the linear mass density 110 tex, filament diameter range from 9 to 12 microns, density of the basalt fibre equal to 2.72 g cm$^{-3}$. Tensile strength on the level of 1870 MPa and elastic modulus in tension of 85 GPa were reported by the manufacturer in the material data sheet. The basalt fibres cannot be used at the maximal application temperature mentioned by manufacturer (i.e. 1000 °C) because a significant degradation (softening) of the fibres even below this limit temperature was previously found.[32] However, for the temperature range used for partial pyrolysis in this investigation mentioned fibres are suitable. Application of two matrix precursors (MS and MPS) led to manufacturing of two sets of composite materials further mentioned as MSC and MPSC. First, the fabric was impregnated with the resin diluted by solvent and then was dried at room temperature. Then the composite plates were manufactured by lamination of manually prepared prepregs. Sixteen layers of prepregs were stacked in the same orientation, by warp, in the longitudinal direction of the mould. Curing was carried out under pressure in a heated mould with controlled temperature and pressure up to 250 °C. During release of the reaction water at the temperature range of 220–250 °C the maximum pressure of 0.86 MPa was applied. The volume fraction of fibres of the cured composite was approximately 43%. Subsequently, all composites were partially pyrolysed using one of targeted temperatures, i.e. the temperature of 600, 650, 700, 750 or 800 °C, in a protective atmosphere of nitrogen. Composite plates with nominal dimensions of 250 mm × 50 mm × 2.5 mm were prepared and cut into the specimens suitable for mechanical testing. Determination of the static flexural strength and measurement of the Young's modulus was carried out by the testing machine Inspekt 100 (Hegewald&Peschke, Germany). Configuration of the measurement corresponds to the standard.[33] The flexural strength was measured in the three-point bending configuration (span of 40 mm) with an inductive extensometer. All static flexural strength tests were carried out using prismatic specimens with nominal dimensions of 50 mm × 8 mm × 2.5 mm and cross-head speed of 1 mm min$^{-1}$. Additionally, the information about the consumed energy during fracture process was calculated from the recorded load deflection traces. The calculated energy was taken as an energy (elastic and plastic) up to the point where force drops of 50% of the reached maximum. Determined work of fracture is thereafter mentioned as $WoF_{50\%F_{max}}$. The 50% drop of the maximal force was selected as a criterion due to the limitation of testing jigs. It was not possible to conduct the test to the total fracture in the most of cases (see Fig. 1). The 50% load drop criterion was selected to allow comparison with the results obtained from the dynamic tests. It is necessary to mention that the consumed energy after this force drop was unknown comparing to the energy consumption during the dynamic loading as will be explained in details in the impact loading section. Further, the normalization of the work of fracture by the sample cross-section allows direct comparison of all obtained values independently on the sample cross-section. For accurate measurement of the Young's and shear modulus in the above mentioned bending samples, a resonant frequency method

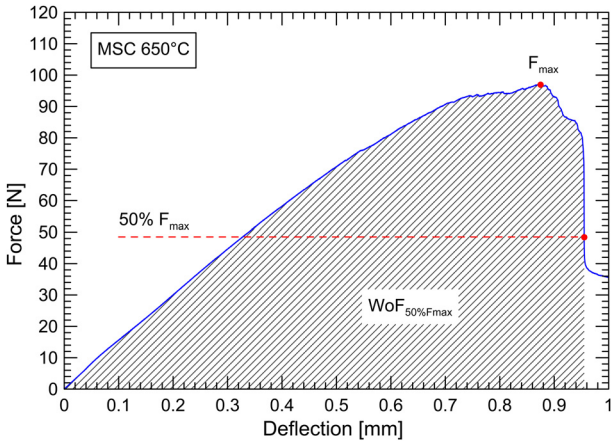


Fig. 1. Typical loading curve for the MSC material prepared at 650 °C with marked area representing work of fracture for 50% force drop.

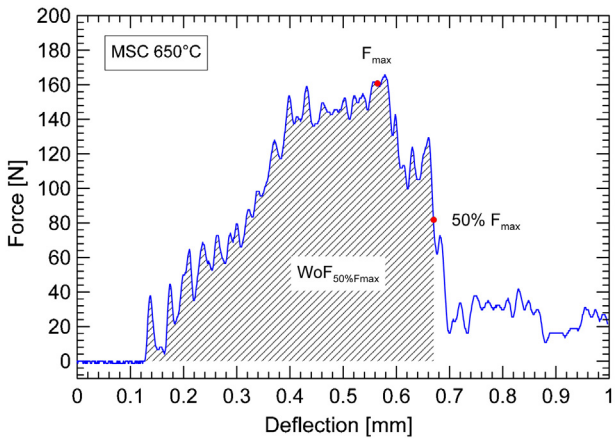


Fig. 2. Typical loading curve for the MSC material prepared at 650 °C for the impact test up to 1 mm of deflection.

was used. Young's modulus was evaluated from the spectrum of longitudinal resonant oscillations. The shear modulus was evaluated according to the spectrum of transverse resonant oscillations with the help of resonant measurement results of Young's modulus. Both measurements were performed on the resonant frequency tester Erudite (CNS Electronics Ltd., UK). Method applied for evaluation of the Young's and the shear modulus is described in.[34,35] The fracture toughness determination using the chevron notch technique on sub-sized specimens based on the standard procedure[36] was conducted. The chevron notch was prepared in the fracture toughness samples by two cuts using precise diamond wheel with thickness of 0.15 mm mounted in a precise saw Isomet 5000 (Buehler, USA). The cross-section of prepared beams was nominally 2.8 mm × 3.7 mm. The three point bending configuration with the span of 16 mm was used for loading in a universal testing machine Zwick Z50 (Zwick/Roell, Germany). Cross-head speed of 10 $\mu$m min$^{-1}$ was used during all tests and the maximum applied force from measured loading curves was used for the fracture toughness calculation. The slice model developed by Bluhm was used for compliance function calculation.[37] The chevron notch depth was determined from the side of the specimen using a travelling microscope (Mitutoyo, Japan) before loading because it was found that in some cases (especially at lower pyrolysis temperatures 600 and 650 °C) it was not possible to obtain this information post mortem from the fracture surface. However, if it was possible, the chevron notch depth for the fracture toughness calculation was taken primarily from the measurement on the fracture surface obtained by an image analysis with higher precision. The fracture toughness values in the perpendicular direction to the fabric plane with edgewise oriented sample (i.e. in-plane direction) to the loading force was determined. Application of the chevron notch in fibre reinforced composites is usually the only method for fracture toughness determination and results have to be evaluated with respect to all limits of this method (see [38–40]). Determination of the resistance to the impact loading was conducted in the in-plane sample orientations using an instrumented impact tester B5113.303 (Zwick/Roell, Germany) with the maximum hammer energy capacity of 15 J. The possibility to set various release angle allows to adjust preciously the impact velocity which was set to 1 m s$^{-1}$, i.e. release angle of 30°. The speed was set on the upper limit where the loading curve is still realistic and the inertia dynamic effects are on the acceptable level as was found previously for brittle materials.[41] The recorded force deflection traces were used for determination of the dynamic flexural strength calculated from the maximum force and the energy used during the fracture process. An example of the typical loading curve in comparable deflection corresponding to the static loading (i.e. up to deflection of approximately 1 mm or up to the first significant drop of the loading force) is shown in Fig. 2 for the MSC material prepared at 650 °C. The work of fracture was determined by the same approach used for static loading described earlier. In some cases the applied force did not reach the zero level in this first fracture stage and fracture process continues further. An example of the full length loading curve up to the point when force drops to zero can be seen in Fig. 3. According to the instrumented impact tester principle it was possible to determine a total consumed energy directly from the hammer position before and after the test which corresponds to the area under the loading curve. The energy consumption analysis was

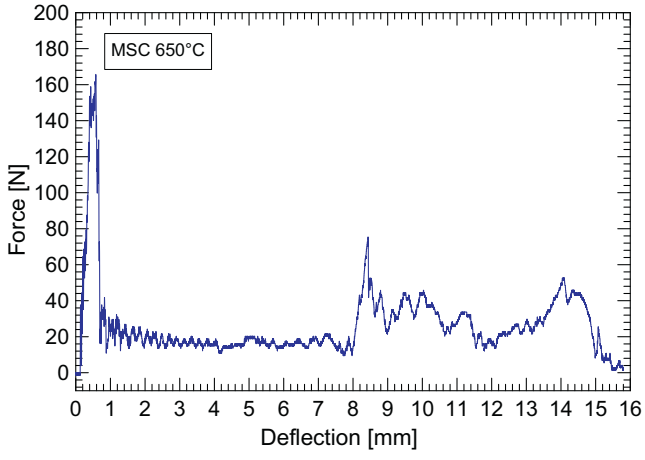


Fig. 3. Typical loading curve for the MSC material prepared at 650 °C for the impact test up to the drop of the force to zero.

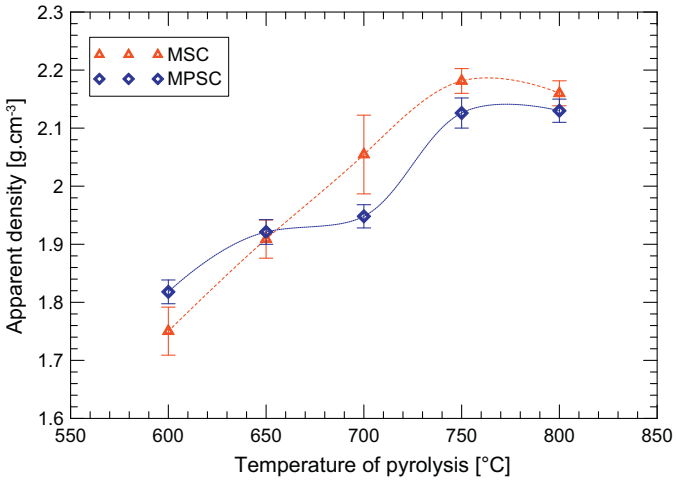


Fig. 4. The apparent density dependence on the temperature of pyrolysis for both the MSC and the MPS composite materials.

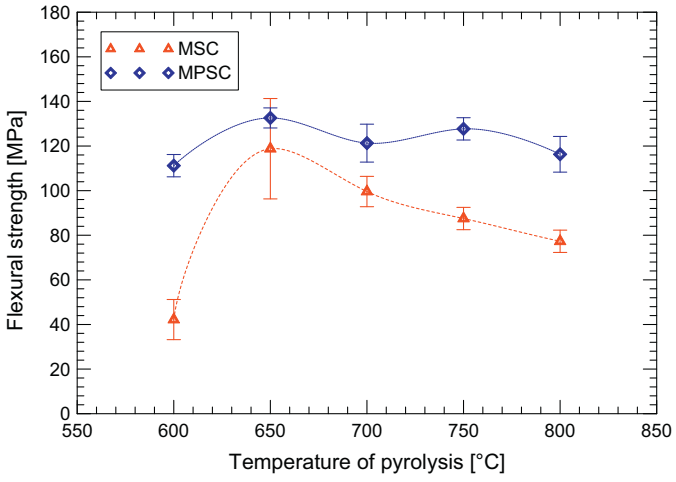


Fig. 6. The dependence of four-point bending flexural strength on the temperature of pyrolysis for both the MS and the MPS composite materials.

therefore divided to the comparison of the first part of the loading curve between static and dynamic loading and to the energy consumption counting fracture processes after the 50% force drop criterion. Additionally, a high speed camera i-SPEED 3 (Olympus, Japan) was used to record an images sequence of the fracture process with the frame rate of 50,000 frames $s^{-1}$. The recorded videos (images sequences) were used for subsequent qualification of changes taking place in the fracture process of various composites and sample orientations. Observation of the fracture surfaces after experiments was conducted using a Lyra 3 XMU FEG/SEM (Tescan, Czech Republic).

## 3. Results and discussion

The apparent density of prepared composite materials was evaluated on the samples cut from the plate using the geometry and weight data. The course of apparent density development in dependence on the temperature of pyrolysis together with the scatter of the measurements is shown in Fig. 4 where similar trends are expressed by dashed and dotted spline lines for both MS and MPS types of composites. There is a visible increase of the density with increasing temperature of pyrolysis up to the temperature of 750 °C where after the densification it does not seem to be very extensive. The trend in case of the MSC material is linear in the first region (up to 750 °C) while the MPSC material exhibits a step at 650 °C where densification slows down, however, the density obtained at 700 °C can be influenced by even small changes in the fibre volume ratio of the evaluated sample. Observed global trend of increasing density with increase of the pyrolysis temperature is connected to the transformation of polymeric precursor to the amorphous SiOC glass which is accompanied by the shrinkage and by the release of gaseous products. The microstructure of all composites seems to be fully compact except the MSC composite prepared at 600 °C where the matrix is not fully compacted especially on the interfaces between individual layers of prepregs. In some cases cracks in the matrix as a consequence of shrinkage at both composites pyrolysed at 600 and 650 °C were present. These

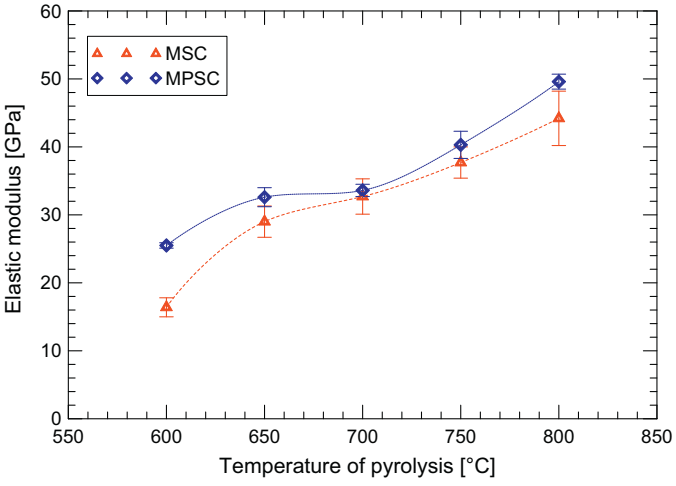


Fig. 5. The dependence of elastic modulus determined from the flexural strength test on the temperature of pyrolysis for both the MS and the MPS composite materials with scatter bars.

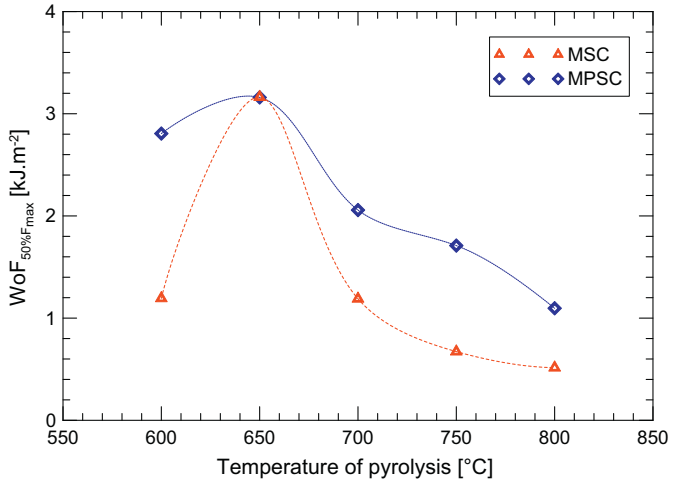


Fig. 7. The dependence of work of fracture values determined from the four-point bending flexural test on the temperature of pyrolysis for both the MS and the MPS composite materials.

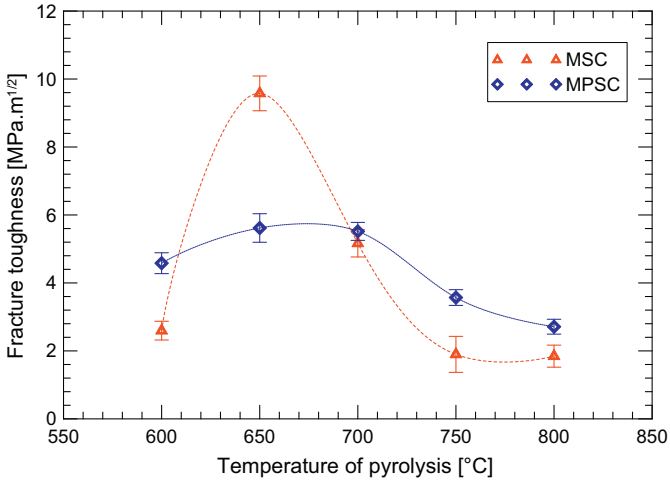


Fig. 8. The dependence of fracture toughness on the temperature of pyrolysis for both the MS and the MPS composite materials.

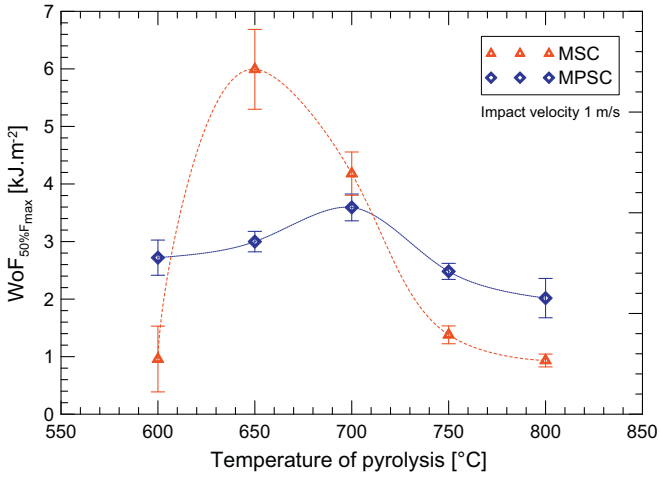


Fig. 10. The dependence of work of fracture ($WoF_{50\%F_{max}}$) values determined from the impact test on the temperature of pyrolysis for both the MS and the MPS composite materials.

processing cracks were transformed to the pores form (i.e. the crack tip was blunted) when the higher temperatures of pyrolysis were applied. The elastic modulus determined from the loading curves obtained during the flexural strength test was determined from the slope of the linear onset of applied force and sample dimensions according to the standard.[35] The obtained average values together with scatter bands are plotted in Fig. 5 and trends are shown by dashed and dotted spline lines. The elastic modulus values reflect naturally the degree of polymer transformation where the maximum values exceed 50 GPa only for MPSC prepared at 800 °C and the obtained trends are in good agreement with the apparent density development. The flexural strength average values determined from the maximal force during loading in the four-point bending configuration together with corresponding standard deviation is plotted in Fig. 6. Taking into account the scatter of the flexural strength the values obtained for the individual MPSC materials is rather on the same level of 120 MPa (see the diamond symbols). The different situation can be observed in the MSC material where strong onset of the flexural strength values is observed between temperatures of 600 °C and 650 °C reaching the maximum, close to the level typical for the MPSC, followed by slight decrease to the level of 80 MPa for the temperature of pyrolysis of 800 °C. From this trend which does not correspond neither to the development of density nor the course of the elastic modulus (see Figs. 4 and 5) it can be pointed out that the bonding between fibres and matrix plays a significant role as well as presence of micro cracking developed in the matrix by its shrinkage. The flexural strength development is useful characteristic in case of brittle monolithic materials but in the case of composites it can be meaningless because it is not able to describe the fracture process in composite materials sufficiently. However, obtained flexural strength values are important from the design point of view. Many authors deal with an another quantity, the work of fracture, which is in principle the amount of energy necessary to break the material. This characteristic or similar energetic criterion is suitable to compare composites to each other. It will be shown further

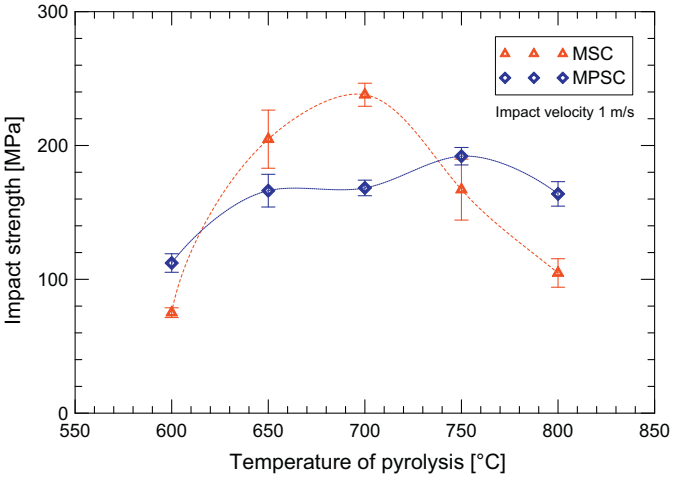


Fig. 9. The dependence of impact strength on the temperature of pyrolysis for both the MS and the MPS composite materials.

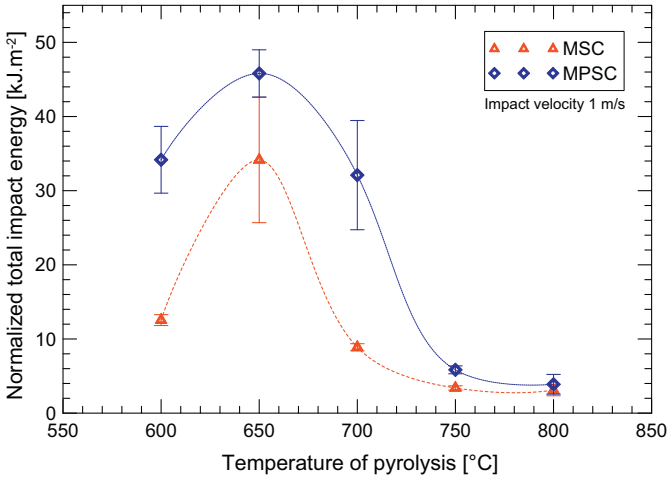


Fig. 11. The dependence of normalized total used energy during the impact loading on the temperature of pyrolysis for both the MS and the MPS composite materials.

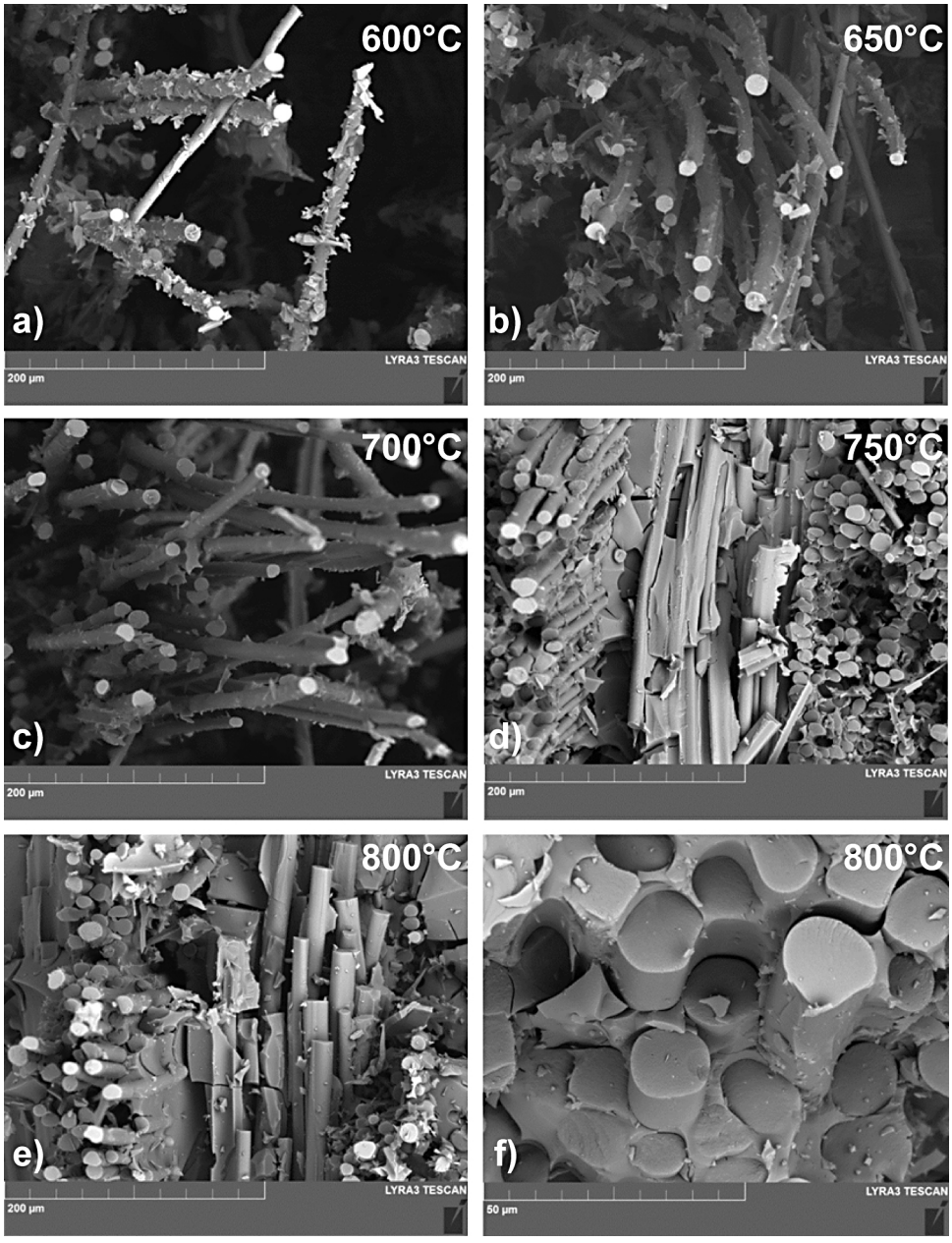


Fig. 12. The overview of fracture surfaces showing development of pull-out mechanism with increasing pyrolysis temperature for the MPSC material.

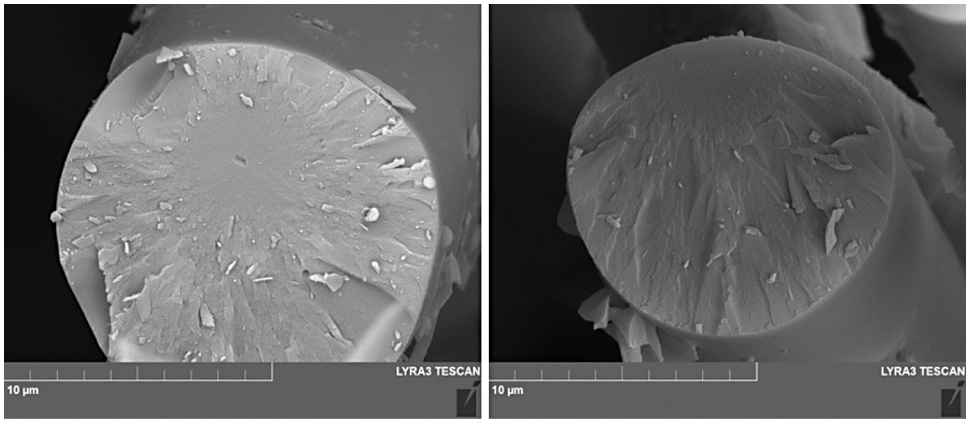


Fig. 13. Examples of typical fracture of fibres for MPSC material prepared at 700 °C where the fracture origin was located in the central part of fibre (left) and on the fibre surface (right).

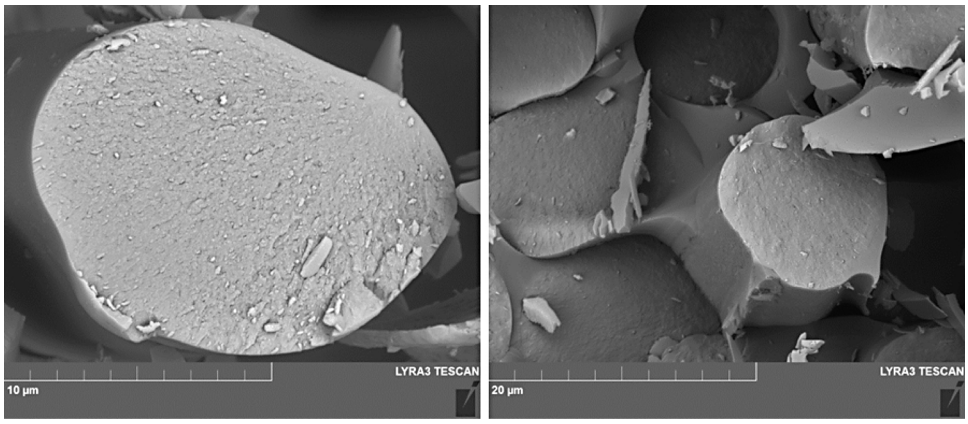


Fig. 14. Examples of typical fracture patterns of fibres for the MPSC material prepared at 750 °C (left) and for the MSC material pyrolysed at 800 °C (right).

when results from impact experiments will be discussed that such energy can additionally explain the efficiency of toughening mechanisms acting during the fracture process. The whole fracture energy in the case of static loading is problematic to determine. This can provide a qualitative comparison and main trends are outlined in Fig. 7. It can be concluded, that the flexural strength reflects only the maximal stress occurring on the surface of sample, but is not able to cope with fracture process itself. From obtained information it is obvious, that the pyrolysis temperature of 650 °C is the optimum processing condition with the highest fracture resistance for both composites under the investigation. The MPSC material has a higher fracture resistance measured by the energy consumption compared to the MSC for all temperatures of pyrolysis. There can be seen a slight discrepancy with fracture toughness data measured by chevron notch technique shown in Fig. 8 where the MSC material exhibits significantly higher value than the MPSC at pyrolysis temperature of 650 °C. The main reason can be attributed to the direction of crack propagation, where for the fracture toughness test it was measured in orientation "out-of-plane" while the bending test was conducted under "in-plane" sample orientation. Crack propagation directions are in both cases perpendicular to the woven fabric plane, however, the in plane sample orientation allows delamination along the fibres in both directions. Dynamic

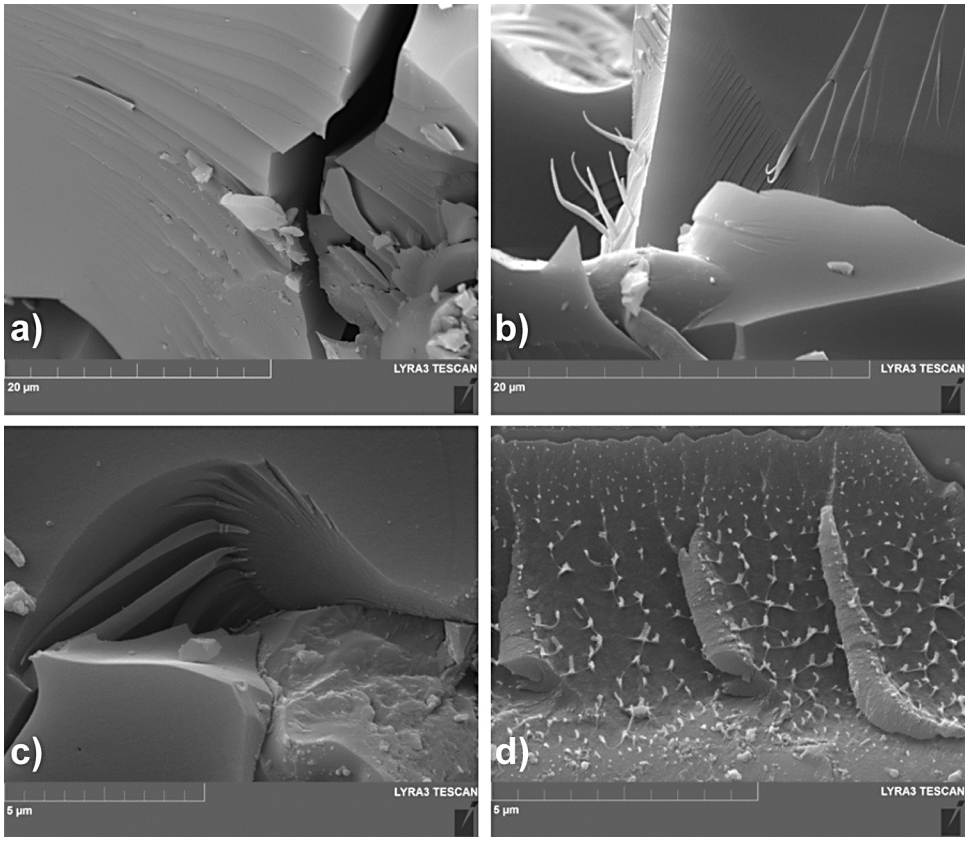


Fig. 15. The examples of typical fracture patterns of the matrix found for MPSC material treated at 750 °C for (a) static loading and (b–d) dynamically loaded specimens.

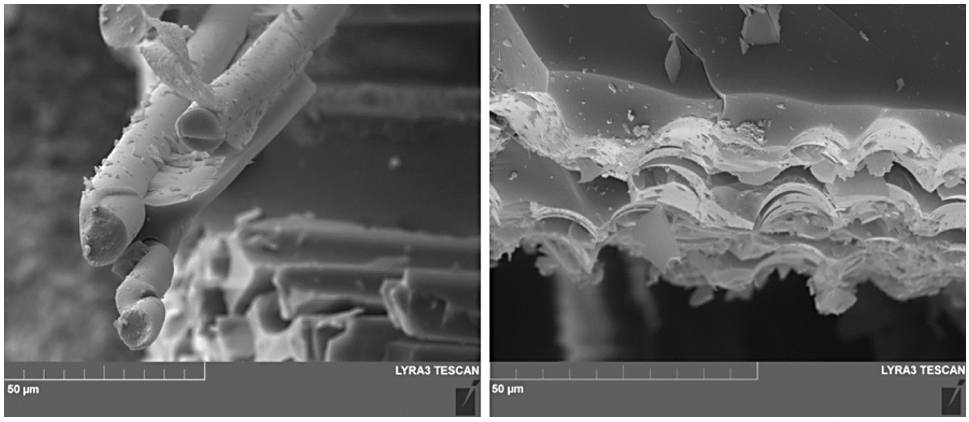


Fig. 16. Multiple fracture of dynamically loaded fibres for MPSC material.

loading was conducted in the same sample orientation as for the static bending test. The main difference was in the loading configuration where the three point bending configuration for dynamic loading was used instead of static four point bending. Therefore, higher values of strength were expected. The dependence of the impact strength on the pyrolysis temperature is plotted in Fig. 9 for both the MSC and the MPSC materials. The MPSC material exhibits a trend similar to that observed in the case of static loading. The level of impact strength for the MPSC material is only slightly changed with the pyrolysis temperature. The MSC material has changed the trend completely when compared with static results because the maximum strength was not reached at the pyrolysis temperature of 700 °C rather 650 °C. Additionally, the impact strength values of the MSC material treated at the temperature of pyrolysis 650 and 700 °C is higher than the values for MPSC in the same temperature range. The work of fracture determined up to the 50% force drop is plotted in Fig. 10 where similar trends as those observed for static loading can be found. The comparison shows, together with image information from the fast camera, that the first loading region observed is connected to the (i) catastrophic failure of the whole sample cross-section, (ii) fracture of the first outer layer followed by the delamination along the prepreg's plane. In some cases a difference between $WoF_{50\%F_{max}}$ and the total consumed energy can be expressed. The total impact energies consumed during the fracture process were calculated and normalized values by the sample cross-section are shown in Fig. 11. There is the obvious trend, similar to the trend obtained from the static experiments, where for whole temperature range the MPSC materials preserve higher consumed fracture energy. Therefore also higher fracture resistance comparing to the MSC is observed. The values of impact strength describe only the peak values but the energy covers all fracture processes together and seems to be more relevant characteristic for materials under investigation. The fractographic analysis provided an evidence of changed fracture behaviour for different stages of polymer-to-ceramic transformation. The set of SEM images taken from the fracture surface of MPSC material shown in Fig. 12 clearly demonstrates these changes. The temperature of pyrolysis 600 °C leads to the presence of micro-cracking in the matrix due to shrinkage and its low stiffness caused by low ratio of precursor decomposition allows the fibres extremely long pull-out in order of millimetres without significant friction between fibres and matrix. The matrix is not transferring the load properly, which causes low strength of this material. The MPSC material was more fracture resistant than the MSC one, thanks to the small increase of stiffness indicated by increased density. The temperatures of pyrolysis higher than 700 °C led to the subsequent elimination of the effect of pull-out toughening micro-mechanism due to stronger interface bonding between fibre and matrix and it's strengthening. The fracture of strongly bonded fibres embedded in the stiff and brittle matrix generally results in the fracture behaviour which is closer to the monolithic ceramics as can be seen in Fig. 12f) in close detail. The fracture behaviour of the MSC material was very similar to the MPSC one only the slight difference was observed in the lower intensity of pull-out mechanism at higher temperatures of pyrolysis what is in good correlation with the measured apparent density indicating the level of precursor transformation. The pull-out toughening mechanism is generally composed of the following subsequent steps: the elastic crack bridging, fibre matrix delamination, fracture of the fibre and finally pull-out of the fibre. In both MSC and MPSC materials the presence of fracture patterns reveals the fracture origin on the individual fibres and indicates that the fibres were fractured in tension or combination of tension and bending as can be seen in Fig. 13 when the temperature of pyrolysis was lower or equal to 700 °C. Higher level of pyrolysis led to the clamping of fibres by stiffer matrix and additionally also to stronger bonding on the fibre matrix interface. These factors all together influenced also the fracture mechanism of individual fibres where no clear fracture origin can be found as it is illustrated in Fig. 14. The increased loading speed to the velocity of 1 m s$^{-1}$ (i.e. the strain rate on the level of $10^{-3}$ s$^{-1}$) influenced the fracture behaviour seriously. As it was reported earlier, the energy consumption during the fracture process increased at least ten times and the strength was doubled when comparing both impact and static loading. The origin of this increase in the fracture resistance can be explained by the changes in the fracture of matrix and also in fibres, which is slightly different from the static loading. The matrix exhibits brittle fracture with the presence of typical features for ceramic or glass materials as is shown in Fig. 15(a). No evidence of plastic behaviour is

present, despite the matrix not being fully transformed to the silicon oxycarbid glass, when static loading is applied. Opposite situation can be observed in the case of dynamic loading. The micrograph in Fig. 15(b) and (c) illustrates the fractured matrix where on the fracture surface an indication of plastic behaviour can be seen in the form of small needle like objects clearly visible on the left side. The other sign of plastic behaviour is displayed in Fig. 15(d) where a network of plastically deformed areas is present. All plastically deformed parts consumed more energy comparing to the cleavage fracture of the matrix observed in the statically loaded composites. Additionally, the excess of energy during impact loading caused also multiple fractures of fibres as is demonstrated in the Fig. 16.

## 4. Conclusions

The set of the basalt woven fabric reinforced hybrid composite materials was prepared using cheap raw materials with the aim to obtain an optimum strength to fracture toughness ratio and to determine changes in the fracture behaviour together with the degree of polymer-to-ceramic transformation. The optimum processing parameters were established for the pyrolysis temperature of 650 °C where the best mechanical properties were found. The MPSC material exhibits higher static flexural strength and total fracture energy in comparison with the MSC material. Fractographic analysis revealed acting toughening mechanisms and their changes with the changed temperature of pyrolysis. The dominant toughening mechanism was identified as the fibre pull-out. During the impact loading the total fracture energy was measured to be ten times higher than the work of fracture determined from the loading curve up to the first 50% force drop for both static and dynamic loading. The impact strength was doubled for both materials under investigation compared to static flexural strength. The reason for the described increase of the fracture resistance for dynamic loading was identified as presence of multiple fibre fracture and the occasional plastic behaviour of the matrix.

## Acknowledgements

This work was realised in CEITEC – Central European Institute of Technology with research infrastructure supported by the project CZ.1.05/1.1.00/02.0068 financed from European Regional Development Fund and financially supported by Czech Science Foundation project no. GAP107/12/2445.

## References

1. Calard V, Lamon J. A probabilistic-statistical approach to the ultimate failure of ceramic–matrix composites-part I: experimental investigation of 2d woven sic/sic composites. *Compos Sci Technol* 2002;**62**(3):385–93.
2. Lamon J, Thommeret B, Percevault C. Probabilistic-statistical approach to matrix damage and stress–strain behavior of 2-d woven sic/sic ceramic matrix composites. *J Eur Ceram Soc* 1998;**18**(13):1797–808.
3. Goto K, Kagawa Y. Fracture behaviour and toughness of a plane-woven sic fibre-reinforced sic matrix composite. *Mater Sci Eng A* 1996;**211**(1-2):72–81.
4. Mouchon E, Colomban P. Oxide ceramic matrix/oxide fibre woven fabric composites exhibiting dissipative fracture behaviour. *Composites* 1995;**26**(3):175–82.
5. Dong R, Hirata Y, Sueyoshi H, Higo M, Uemura Y. Polymer impregnation and pyrolysis (PIP) method for the preparation of laminated woven fabric/mullite matrix composites with pseudoductility. *J Eur Ceram Soc* 2004;**24**(1):53–64.
6. Lee SH, Weinmann M, Aldinger F. Processing and properties of c/si–b–c–n fiber-reinforced ceramic matrix composites prepared by precursor impregnation and pyrolysis. *Acta Mater* 2008;**56**(7):1529–38.
7. Lange FF, Tu WC, Evans AG. Processing of damage-tolerant, oxidation-resistant ceramic matrix composites by a precursor infiltration and pyrolysis method. *Mater Sci Eng A* 1995;**195**(0):145–50.
8. Miracle DB, Donaldson SL. *ASM Handbook, vol. 21 – Composites*. ASM International; 2001. http://ims.asminternational.org/portal/site/ims/AsmStore/ProductDetails/?vgnextoid=d56253501f0f8110VgnVCM100000701e010aRCRD#details
9. Alsayed S, Al-Salloum Y, Almusallam T, El-Gamal S, Aqel M. Performance of glass fiber reinforced polymer bars under elevated temperatures. *Composites B Eng* 2012;**43**(5):2265–71.
10. Halasova M, Chlup Z, Strachota A, Cerny M, Dlouhy I. Mechanical response of novel sioc glasses to high temperature exposition. *J Eur Ceram Soc* 2012;**32**(16):4489–95.
11. Xu T, Ma Q, Chen Z. Mechanical property and microstructure evolutions of cf/sioc composites with increasing annealing temperature in reduced pressure environment. *Ceram Int* 2012;**38**(1):605–11.
12. Renlund GM, Prochazka S, Doremus RH. Silicon oxycarbide glasses. 1. Preparation and chemistry. *J Mater Res* 1991;**6**(12):2716–22.
13. Renlund GM, Prochazka S, Doremus RH. Silicon oxycarbide glasses. 2. Structure and properties. *J Mater Res* 1991;**6**(12):2723–34.
14. Chlup Z, Cerny M, Strachota A, Kozak V. Properties of modified polysiloxane based ceramic matrix for long fibre reinforced composite materials. *Plast Rubber Compos* 2011;**40**(6-7):380–5.
15. Duan L, Ma Q. Effect of pyrolysis temperature on the pore structure evolution of polysiloxane-derived ceramics. *Ceram Int* 2012;**38**(4):2667–71.
16. Duan L, Ma Q, Chen Z. Preparation and characterization of mesoporous silicon oxycarbide ceramics without free carbon from polysiloxane. *J Eur Ceram Soc* 2013;**33**(4):841–6.
17. Davis JB, Lofvander JPA, Evans AG, Bischoff E, Emiliani ML. Fiber coating concepts for brittle–matrix composites. *J Am Ceram Soc* 1993;**76**(5):1249–57.
18. Perez-Rigueiro J, Celemin J, Llorca J, Herrero P. Oxidation of bn/nicalon fiber interfaces in ceramic-matrix composites and its effect on fiber strength. *J Am Ceram Soc* 1999;**82**(12):3494–500.
19. Kaya C, Kaya F, Boccaccini AR, Chawla KK. Fabrication and characterisation of Ni-coated carbon fibre-reinforced alumina ceramic matrix composites using electrophoretic deposition. *Acta Mater* 2001;**49**(7):1189–97.
20. Kaludjerovic BV, Kljajevic LM, Lausevic ZV. The effect of partially carbonized fibers on the mechanical properties of carbon/carbon composites. *J Mater Process Technol* 2012;**212**(1):157–63.
21. Chlup Z, Cerny M, Strachota A, Dlouhy I, Sandera P. Role of pyrolysis conditions on fracture behaviour of fibre reinforced composites. *Mater Struct Micromech Fract* 2011;**465**:455–8.
22. Strachota A, Cerny M, Chlup Z, Slouf M, Hromadkova J, Plestil J, et al. Optimization of sol–gel/pyrolysis routes to silicon oxycarbide glasses. *J Non-Cryst Solids* 2012;**358**(20):2771–82.
23. Cerny M, Sucharda Z, Strachota A, Chlup Z, Glogar P. Influence of the organic/inorganic pyrolysis conversion level on mechanical properties of composites with e-glass or basalt fibre reinforcement. *Ceramics-Silikaty* 2010;**54**(4):345–51.
24. Supova M, Svitilova J, Chlup Z, Cerny M, Weishauptova Z, Suchy T, et al. Relation between mechanical properties and pyrolysis temperature of phenol formaldehyde resin for gas separation membranes. *Ceramics-Silikaty* 2012;**56**(1):40–9.

25. Shanan Moore Stevens N, Rezac ME. Formation of hybrid organic/inorganic composite membranes via partial pyrolysis of poly(dimethyl siloxane). *Chem Eng Sci* 1998;**53**(9):1699–711.
26. Trick KA, Saliba TE. Mechanisms of the pyrolysis of phenolic resin in a carbon/phenolic composite. *Carbon* 1995;**33**(11):1509–15.
27. Cerny M, Strachota A, Chlup Z, Sucharda Z, Zaloudkova M, Glogar P, et al. Strength, elasticity and failure of composites with pyrolyzed matrices based on polymethylsiloxane resins with optimized ratio of d and t components. *J Compos Mater* 2013;**47**(8):1055–66.
28. Cerny M, Glogar P, Sucharda Z, Chlup Z, Kotek J. Partially pyrolyzed composites with basalt fibres – mechanical properties at laboratory and elevated temperatures. *Composites A Appl Sci Manuf* 2009;**40**:1650–9.
29. Chawla N, Chawla KK, Koopman M, Patel B, Coffin C, Eldridge JI. Thermal-shock behavior of a Nicalon–fiber-reinforced hybrid glass–ceramic composite. *Compos Sci Technol* 2001;**61**(13):1923–30.
30. Dlouhy I, Chlup Z, Chawla K, Kulkarni R, Koopman M, Boccaccini A. Effect of static pre-loading on fracture toughness of Nicalon (r) fibre glass matrix composite. *Mater Sci Eng A Struct Mater Properties Microstruct Process* 2004;**367**(1–2):17–23.
31. Dlouhy I, Kotoul M, Vyslouzil T, Chlup Z, Boccaccini A. Crack resistance curve in glass matrix composite reinforced by long Nicalon (r) fibres. *J Mater Sci* 2008;**43**(12):4022–30.
32. Cerny M, Glogar P, Golias V, Hruska J, Jakes P, Sucharda Z, et al. Comparison of mechanical properties and structural changes of continuous basalt and glass fibres at elevated temperatures. *Ceramics-Silikaty* 2007;**51**:82–8.
33. *843-1, E. Advanced Technical Ceramics. Mechanical Properties of Monolithic Ceramics at Room Temperature. Determination of Flexural Strength*; 2007.
34. Cerny M, Glogar P, Manocha LM. Resonant frequency study of tensile and shear elasticity moduli of carbon fibre reinforced composites (CFRC). *Carbon* 2000;**38**(15):2139–49.
35. *843-2, E. Advanced Technical Ceramics – Mechanical Properties of Monolithic Ceramics at Room Temperature – Part 2: Determination of Young's Modulus, Shear Modulus and Poisson's Ratio*; 2006.
36. *EN14425-3. Advanced Technical Ceramics – Test Methods for Determination of Fracture Toughness of Monolithic Ceramics – Part 3: Chevron Notched Beam (CNB) Method*; 2010.
37. Bluhm JI. Slice synthesis of a three dimensional "work of fracture" specimen. *Eng Fract Mech* 1975;**7**(3):593–604.
38. Boccaccini AR, Rawlings RD, Dlouhý I. Reliability of the chevron-notch technique for fracture toughness determination in glass. *Mater Sci Eng A* 2003;**347**(1–2):102–8.
39. Dlouhy I, Boccaccini AR. Reliability of the chevron notch technique for fracture toughness determination in glass composites reinforced by continuous fibres. *Scr Mater* 2001;**44**(3):531–7.
40. Dlouhy I, Chlup Z, Atiq S, Boccaccini A, Bradt R, Munz D, et al. Fracture resistance of hybrid glass matrix composite and its degradation due to thermal ageing and thermal shock. *Active Mater Nanoscale Mater Composites Glass Fundam* 2005;**14**:263–74.
41. Chlup Z, Flasar P, Dlouhy I. Response of inherently brittle materials on higher loading rates. *Eng Fract Mech* 2010;**77**(2):359–66.